Observations of the methanol 4_{-1}-3_0 E line in molecular clouds

I. I. Berulis [a] , S. V. Kalenski [a] , A. M. Sobolev [b] & V. S. Strelnitski [c]

[a] Astro-Space Center , Lebedev Physical Institute , 84/32 Profsojusnaja Str., Moscow, 117810, USSR

[b] Astronomical Observatory , Urals State University , 51 Lenin Ave., Sverdlovsk, 620083, USSR

[c] Institute of Astronomy , 48 Pjatnitskaja Str., Moscow, 109017, USSR
Published online: 12 Nov 2007.

PLEASE SCROLL DOWN FOR ARTICLE

representations or warranties whatsoever as to the accuracy, completeness, or suitability for any purpose of the Content. Any opinions and views expressed in this publication are the opinions and views of the authors, and are not the views of or endorsed by Taylor & Francis. The accuracy of the Content should not be relied upon and should be independently verified with primary sources of information. Taylor and Francis shall not be liable for any losses, actions, claims, proceedings, demands, costs, expenses, damages, and other liabilities whatsoever or howsoever caused arising directly or indirectly in connection with, in relation to or arising out of the use of the Content.

This article may be used for research, teaching, and private study purposes. Any substantial or systematic reproduction, redistribution, reselling, loan, sub-licensing, systematic supply, or distribution in any form to anyone is expressly forbidden. Terms & Conditions of access and use can be found at http://www.tandfonline.com/page/terms-and-conditions

OBSERVATIONS OF THE METHANOL 4_{-1}–$3_0\,E$ LINE IN MOLECULAR CLOUDS

I. I. BERULIS and S. V. KALENSKI

Astro-Space Center, Lebedev Physical Institute, 84/32 Profsojusnaja Str., Moscow 117810, USSR

A. M. SOBOLEV

Astronomical Observatory, Urals State University, 51 Lenin Ave., Sverdlovsk 620083, USSR

and

V. S. STRELNITSKI

Institute of Astronomy, 48 Pjatnitskaja Str., Moscow 109017, USSR

(14 April, 1991)

Searches for new sources and regular monitoring of several molecular clouds in the methanol 4_{-1}–$3_0\,E$ transition are in progress since 1988 with the 22 meter radio telescope of the Lebedev Physical Institute. Spectra and several-point maps (when available) of the sources are presented and briefly discussed. Several sources emit both "broad" (a few km/s) and "spike" (≤ 1 km/s) spectral features. No time variations were detected within the accuracy of the observations. The common procedure of the methanol column density calculations for the "broad" 4_{-1}–$3_0\,E$ features is critically analyzed. It is shown that treating these features as optically thin and "thermal" may lead to an over estimation of the column density by the order of magnitude. The astrophysical nature of the "broad" and "spike" components is discussed.

KEY WORDS Interstellar methanol, molecular clouds, radio lines.

1. INTRODUCTION

Methanol (CH_3OH) is one of the most informative molecules for the observational study of the sites of active star formation. Several of its lines (J_2–$J_1\,E$, 4_{-1}–$3_0\,E$, 5_{-1}–$4_0\,E$, 7_0–$6_1\,A^+$, 8_0–$7_1\,A^+$) are often observed at the same position and the same radial velocities; these lines were categorized as "Class A" lines (Batrla *et al.* (1987), Hashick, Menten and Baan (1990)—hereafter HMB). Though observed in warm (and thus star producing) molecular clouds, Class A lines emitters are not directly associated with such indicators of very young stars as compact HII regions, compact IR sources, H_2O or OH masers. This gives some ground to suppose that these sources may be related to even earlier stages of star formation. Potential possibility of observing the earliest stages of star formation makes the methanol Class A lines particularly interesting.

To search for new sources and to regularly investigate the already known ones (in particular, for their possible time variations), we have undertaken, since 1988, a permanent observational program in $4_{-1}-3_0\,E$ line, at 36.169 GHz, with the Pushtchino 22 meter radio telescope of the Lebedev Physical Institute (Berulis & Ponomarenko, 1988; Berulis *et al.*, 1988; Berulis *et al.*, 1990). We regularly observed the Sgr A, Sgr B2, Ori-KL, W51, DR 21, and NGC 2264 molecular clouds and have made a single observation of W3 OH. We also detected the $4_{-1}-3_0\,E$ emission in one new source, G1.6–0.025. For this source and for Sgr B2, Ori-KL, and W51, several-point offset mapping has been made.

The observational technique is briefly described in section 2, and the results of the observations are presented in section 3. In section 4 we use the results of a numerical simulation for the methanol-*E* rotational levels excitation to discuss the procedure of the methanol column density determination (sub-section 4.1), and we discuss the possible astrophysical nature of the "broad" and "spike" methanol spectral features (sub-section 4.2).

2. OBSERVATIONS

The Pushtchino 22 meter antenna of the Lebedev Physical Institute, augmented with a 8.2 mm maser amplifier receiver, has been used for the observations. The system temperature was $\approx$250 K. There were two parallel spectrometers at the output, with spectral resolutions of 7.5 and 125 kHz, respectively (0.062 and 1.04 km/s, at 36.169 GHz).

Our computer can simultaneously examine 128 spectral channels. This determined the bandwidths. The maximum bandwidth was thus $128 \cdot 125 = 16,000$ kHz, or $\approx$133 km/s. But when both spectrometers were used simultaneously, the bandwidths were $96 \cdot 7.5 = 720$ kHz, or $\approx$6 km/s, for the high-resolution spectrometer, and $(128-96) \cdot 125 = 4000$ kHz, or $\approx$33 km/s, for the low-resolution spectrometer.

The aperture efficiency of the 22 meter antenna at 8 mm is 0.18, and the main beam width (FWHM) is 2 arcmin. The antenna temperature was corrected for atmospheric absorption; 1 K of this corrected antenna temperature corresponds to a flux of 39 Jy. The calibration of the antenna temperature, which was made with a calibrated noise tube, is typically good to $\approx$30%, but is, probably, twice than that worse for low declination sources. The beam switching mode was used for these observations. The pointing errors are estimated to be less than 30 arcsec.

The numerical results of the observations are collected in Table 1. The columns are: the source name; its equatorial coordinates for 1950.0; antenna temperature at the center of a spectral feature, corrected for atmospheric absorption; radial velocity relative to the Local Standard of Rest; linewidth (FWHM); molecular column density (see sub-section 4.1).

3. RESULTS FOR INDIVIDUAL SOURCES

G1.6–0.025. Methanol was first detected in this cloud, near the Galactic Center, by Whiteoak and Peng (1989), who observed here the $2_0-3_{-1}\,E$ line in

Table 1 Parameters, determined from $4_{-1}-3_0$ E methanol observations.

Source	α_{1950} δ_{1950}	T_a, K	V_{lsr} (km/s)	ΔV (km/s)	N_{CH_3OH} (cm^{-2})	Notes
W3 OH	$02^h23^m16^s$ $61°38'\,57''$	0.15 ± 0.03	-46.2 ± 0.2	4.4 ± 0.3	8.7E + 15	
Ori–KL	05 32 47 $-05\ 24\ 15$	0.9 ± 0.2	8.4 ± 0.1	1.8 ± 0.1	1.6E + 16	
NGC 2264	06 38 25 09 32 28	0.5 ± 0.1 0.22 ± 0.1	8.7 ± 0.2 8.0 ± 0.1	3.0 ± 0.2 0.8 ± 0.1	9.3E + 14	e
SGR A–G	17 42 27 $-29\ 04\ 36$	2.0 ± 0.5 4.5 ± 1.5	$-5 \div +25$ 5.7 ± 0.2	4.0 ± 0.2	2.5E + 16	a
SGR B2	17 44 07 $-28\ 20\ 15$	11 ± 1.5 20 ± 1.5	$40 - 95$ 70 ± 0.5	3.5 ± 0.2	4.0E + 17	a d
G1. 6–0.025	17 46 12 $-27\ 33\ 15$	2.0 ± 1.0 3.0 ± 1.0	$40 - 65$ 54.2 ± 0.2	<2	2.0E + 15	a, b, c d
W 51	19 21 25 14 25 10	0.45 ± 0.1	55.3 ± 0.2	7.0 ± 0.3	1.6E + 16	f
	19 21 25 14 24 10	0.2 ± 0.1	56.3 ± 0.5	<1		
	19 21 23 19 24 10	0.25 ± 0.1	53.8 ± 1.0	<2		
DR21 WEST	20 37 08 42 08 46	0.8 ± 0.2	-2.7 ± 0.1	0.42 ± 0.05		
DR21 OH	20 37 14 42 11 20	0.4 ± 0.05	-2.8 ± 0.1	3.5 ± 0.2	3.7E + 15	
	20 37 14 42 12 00	0.3 ± 0.1	0.2 ± 0.1	0.8 ± 0.1		e

[a] Non-gaussian profile.
[b] Column density was determined using contour maps (Figure 10).
[c] Exact position of the peak of brightness is not known.
[d] Exact position of the maser is not known.
[e] The line may consist of several components.
[f] Parameters of the strongest component.

absorption. Following the Sobolev's (1990) suggestion that this cloud could be a $4_{-1}-3_0$ E line emitter, we undertook the observations in 9 points towards the cloud. The emission with the brightness temperatures $T_b \approx 3-8$ K has been detected in 7 points, within the radial velocity interval of 40–65 km/s. The spectra are shown in Figure 1. The maximum antenna temperature in $4_{-1}-3_0$ E line is observed towards the point $\alpha(1950) = 17^h46^m12^s$, $\delta(1950) = -27°33'15''$, where Gardner *et al.* (1985) observed a compact ($\leq 81''$) bright NH_3 clump, but at a significantly different radical velocity, $v_{LSR} = 43$ km/s. (Later, Gardner and Boes (1987) reported the detection, in the same direction, of a larger ($5'$) cloud with a *very different* radial velocity—$v_{LSR} = 165$ km/s; unfortunately, our bandwidth did not cover this velocity to look for $4_{-1}-3_0$ E emission). Figure 1 also shows the spectrum obtained in the direction of another NH_3 clump observed by Gardner *et al.* (1985) (at the offset position $\Delta\alpha = +4'30''$; $\Delta\delta = +1'15''$), and the spectrum, which was taken in direction of the strongest (minimum brightness temperature) absorption in the 2_0-3_{-1} E line, as measured by Whiteoak and Peng (1989) (offset position $+2'45''$; $0'0''$). The broad $4_{-1}-3_0$ E emission has the *full* width of about 10–15 km/s. However, this emission changes in shape and width from one offset point to another, and this is indicative of its blended structure, with the probable widths of a few km/s for the individual "broad" blended components. The shape

G1·6 – 0·025

ΔV = 1·037 KM/S
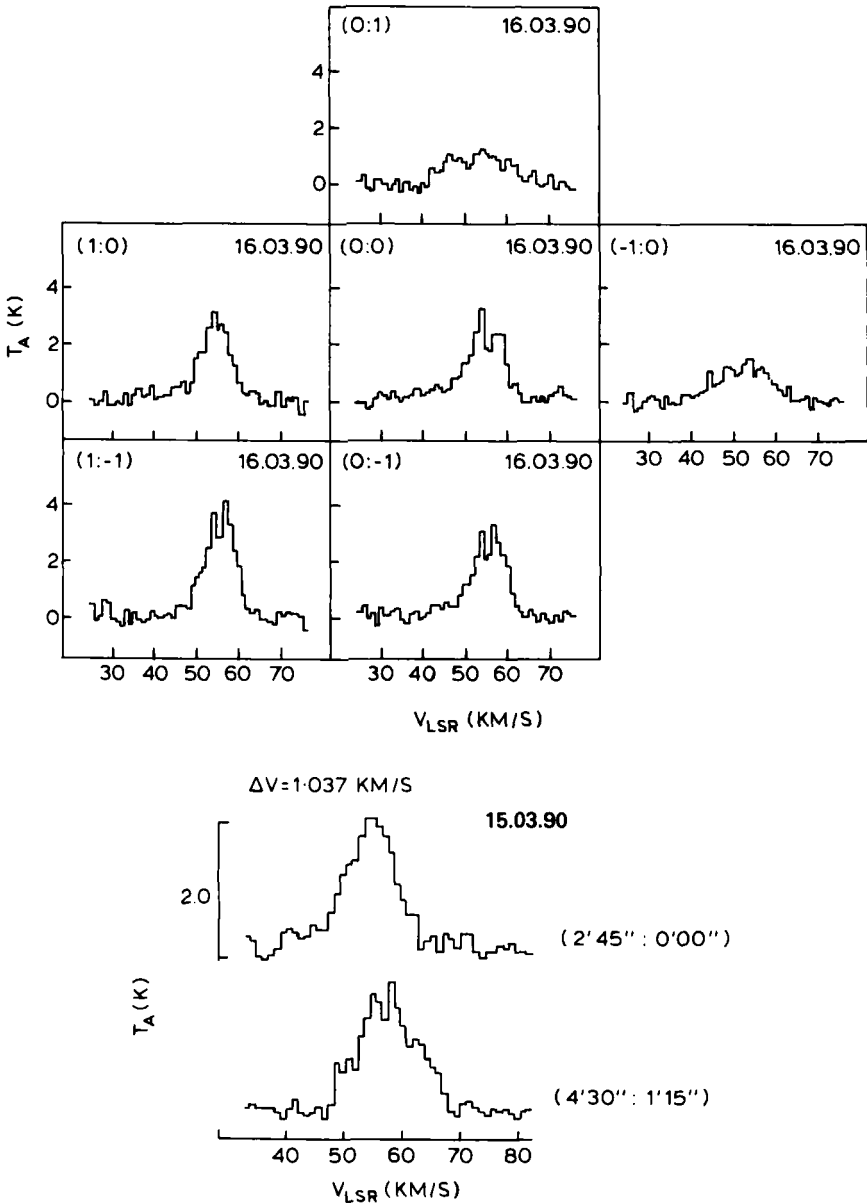
Figure 1 Spectra of G1.6–0.025 in 4_{-1}–3_0 *E*-methanol line. Equatorial coordinates of the central (0; 0) position are given in Table 1. Offset α, δ-positions, in arcmin, and the dates of observations are indicated for each spectrum. Abscissa is for the radial velocity relative to the Local Standard of Rest, and ordinate—for the antenna temperature corrected for atmospheric absorption. Spectral resolution is indicated after the source name.

of the spectrum changes significantly by offsets of 1', and it changes radically, when offsets are larger than 2'. This indicates that the "broad" blended features are produced by clumps with the size scale of the order 1'. Besides these "broad" features there are two narrow (≤ 1 km/s), "spike," features, at $v_{LSR} = 54$ and 57 km/s.

Sgr B2. Spectra of this source at several offset points are shown in Figure 2. In qualitative accordance with Morimoto *et al.* (1985), there is a broad (several tens of km/s) "thermal" background, and narrower "maser" features, one of which, at $v_{LSR} \simeq 70$ km/s, coincides in radial velocity with a "broad maser" feature in Morimoto *et al.* (1985). Unfortunately, any quantitative comparison of our spectra with those by Morimoto *et al.* is impossible because of large pointing and brightness temperature errors due to a very low elevation of the source ($\leq 7°$, at our latitude). Comparison of our own spectra, obtained during the time interval between April 1988 and February 1989, doesn't reveal any change of intensity for the strongest features, within the observational errors.

SGR B2

$\Delta V = 1.037$ (KM/S)
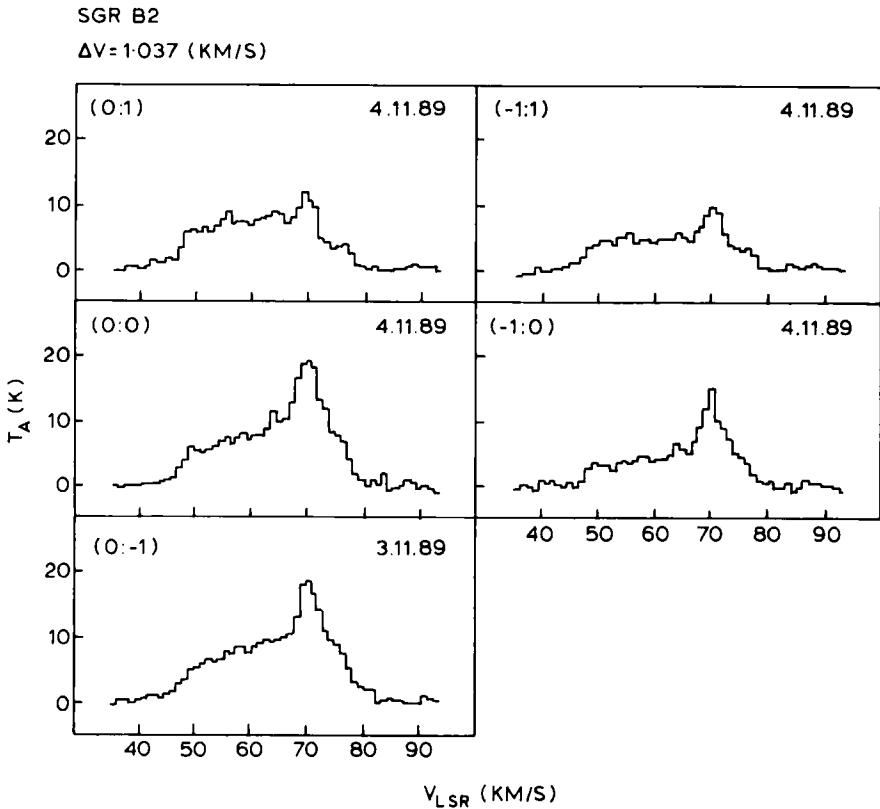
Figure 2 Spectra of Sgr B2. See Table 1, for coordinates of the (0;0) position, and caption to Figure 1 for other comments.

SGR A–G

ΔV = 1·037 KM/S
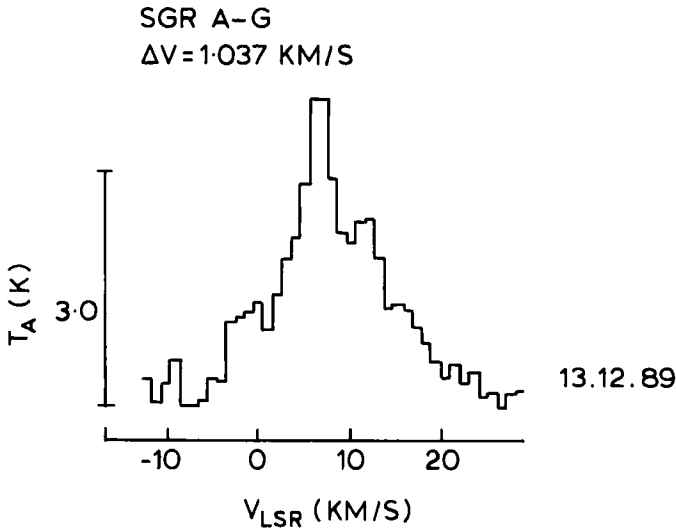
Figure 3   Spectrum of Sgr A–G. See caption to Figure 1 for comments.

Sgr A–G. The $4_{-1}-3_0$ E spectrum of this source (Figure 3) is similar to the Sgr B2 spectrum, though it is weaker and its "thermal" component is narrower. We observed as Hashick and Baan also observed (1989—hereafter HB), besides the broad emission, a narrow component with $\delta v \simeq 4$ km/s. We did not detect any changes surpassing the observational errors between May and December 1989.

Ori-KL. Two spectra of this source, obtained with a time interval of 10 months, are shown in Figure 4a. No detectable change can be noted.

The results of a single-dish mapping in $4_{-1}-3_0$ E line (Figure 4b) suggest that the source is extended for our beamwidth, or multiple. The isophotes are not symmetrical, but there is a pronounced maximum, which coincides, within the pointing errors, with the position of the Methanol Emission Core (MEC) [Johansson *et al.*, 1984; Menten *et al.*, 1988]. The extension of the emission to the South is probably connected with another well-known methanol source, situated at $\simeq 1'.5$ southward of MEC.

Although the source seems extended on our map, the maximum flux density we measured at MEC position ($S \simeq 35$ Jy) is close to the values obtained at the same position by HB and HMB with a beam width of 56″. We conclude that the major contribution to the observed emission at the MEC position makes a region, which is smaller than 1 arcmin in diameter.

W51. Spectra measured on March 14–16, 1990, at 11 positions toward W51 are shown in Figure 5. The source has a complicated structure. One can distinguish at least 2 broad components ($\delta v \simeq 4$ km/s), on which, at some directions, narrow ($\delta v \leq 1.5$ km/s) features are superposed. The narrow features (detected only marginally) coincide in position and velocity, within the measurements errors, with the masers in J_2-J_1 E lines discovered by Menten *et al.* (1986).

DR21 (OH). Our results (Figure 6), like those by HB, revealed a narrow ($\delta v \simeq 0.8$ km/s) feature, superposed on a broader ($\delta v \simeq 4$ km/s) component. No variability was detected between May and October, 1989. Moreover, the flux
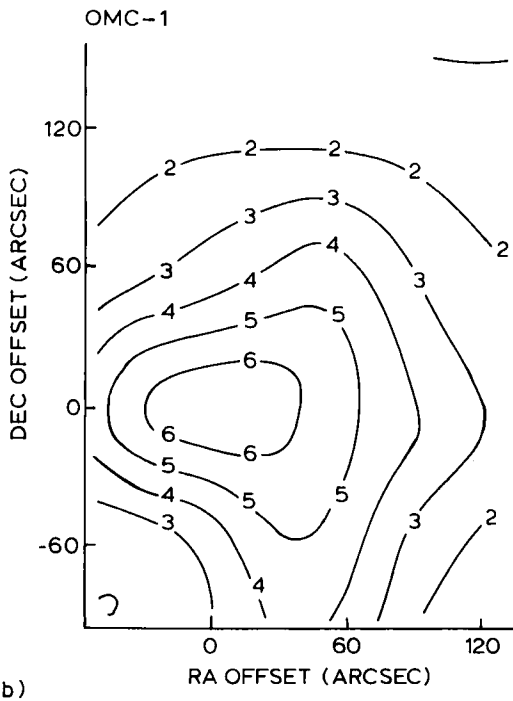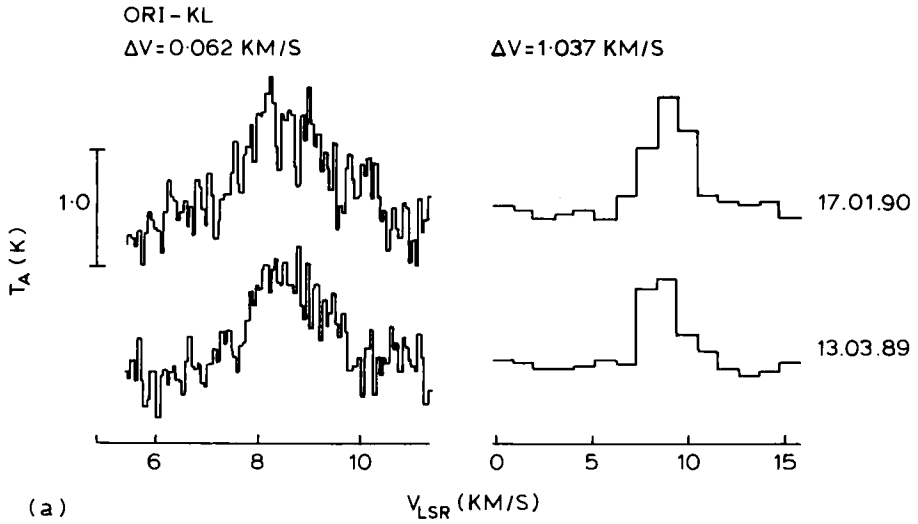
Figure 4 *a*—Spectra of Ori-KL at two dates. See caption to Figure 1 for comments. *b*—A single-dish map of the Ori-KL source in $4_{-1}-3_0$ *E* line. The digits (from 1 to 6) labelling the isophotes correspond to the rising antenna temperature, from $T_A \approx 0.0$ K, with the step 0.15 K. See Table 1 for coordinates of the (0; 0) position.

W51

ΔV = 1·037 KM/S
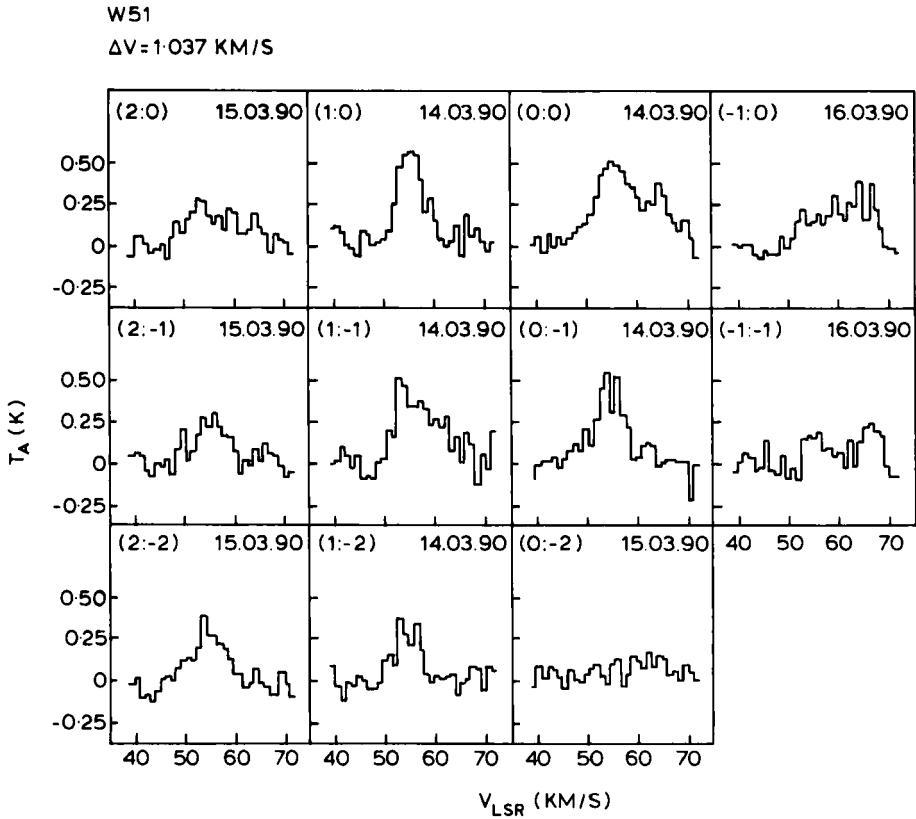
Figure 5 Spectra of W51. See Table 1 for coordinates of the (0; 0) position (55.3 km/s feature) and caption to Figure 1 for other comments.

DR 21 OH

ΔV = 0·062 KM/S   ΔV = 1·037 KM/S
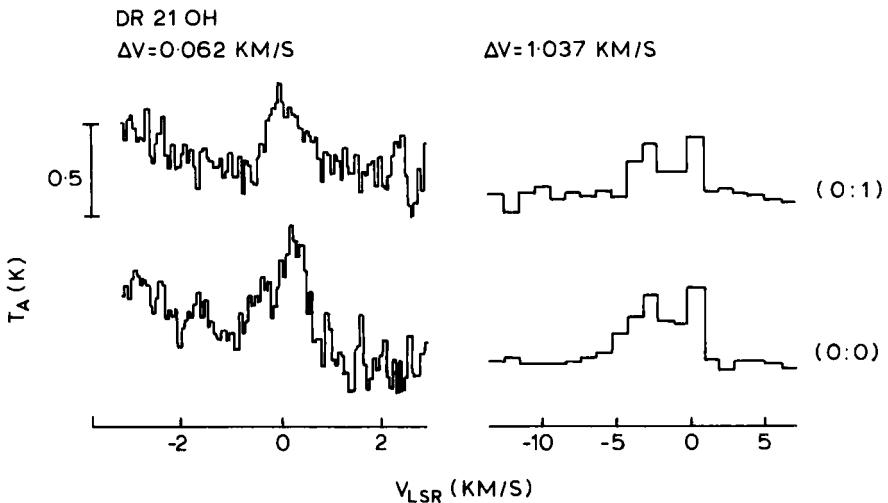
Figure 6 Spectra of DR21 (OH). See caption to Figure 1 for other comments.

DR 21 WEST
ΔV = 0·062 KM/S

13.03.90

V_{LSR} (KM/S)
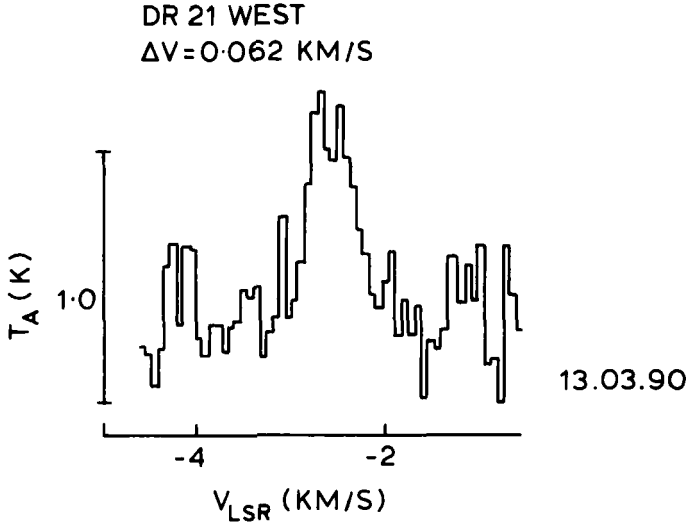
**Figure 7** Spectra of DR21 (West) in the direction $\alpha(1950.0) = 20^h37^m14^s$, $\delta(1950.0) = 42°12'00''$. See caption to Figure 1 for other comments.

density we measured ($\simeq 12\,\text{Jy}$) coincided with that measured by HB. The difference of the narrow component profile shapes, at positions differing by 1' in N–S direction (Figure 6), suggests at least two spatially separated sources.

DR21 (West). We confirmed here (Figure 7) the existence of a narrow line, detected by HMB. A small difference in flux densities, measured by HMB and by us, is probably due to calibration and pointing errors.

NGC 2264. We detected here, at the position of methanol maser, indicated by HB and HMB, a narrow ($\delta v \simeq 0.8\,\text{km/s}$) feature, superposed on a broad

NGC 2264
ΔV = 0·062 KM/S   **ΔV = 1·037 KM/S**

4.05.90

11–12.03.90

V_{LSR} (KM/S)
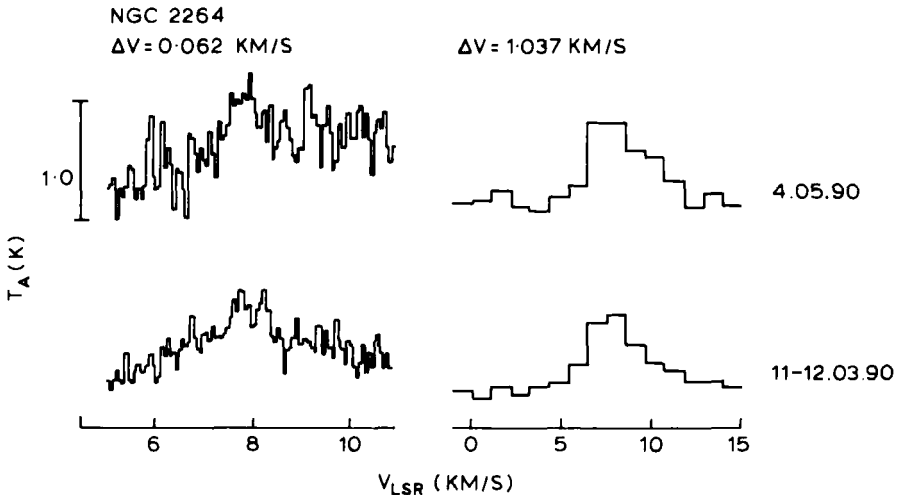
Figure 8 Spectra of NGC 2264. See caption to Figure 1.
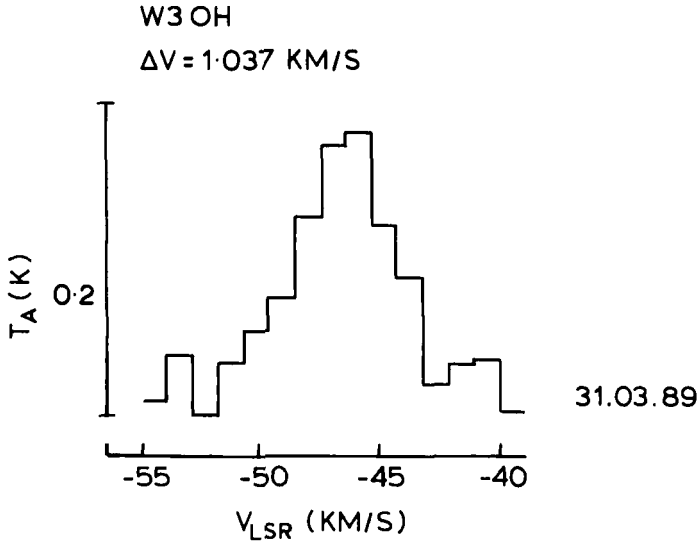
Figure 9   A spectrum of W3 (OH). See caption to Figure 1.

($\delta v \simeq 3$ km/s) component (Figure 8). Our flux measurements are in accordance with the HB and HMB data.

W3 (OH). This is a "Class B" source, according to the classification by Batrla *et al.* (1987). Yet HMB have detected a weak spike in another "Class A" line, 7_0–6_1 A^+. We did not observe any spike in 4_{-1}–3_0 E line, at a level of ≥ 2 Jy, but we did detect a weak broad emission (Figure 9). From the difference of beam-averaged brightness temperatures, deduced by HB and by us, we conclude that the source does not exceed $\simeq 1'$ in diameter.

4. DISCUSSION

4.1. *Column Densities*

It has been known for a long time that the most simple and most probable, collisional-radiative, pumping tends to invert the 4_{-1}–3_0 E methanol transition (for example, Lees, 1973). Sobolev (1990) has shown that this transition should in fact be inverted throughout the possible range of the molecular cloud parameters, unless the cloud is subject to a stronger exterior IR irradiation. In few cases, where it is possible to estimate the cloud's size, the excessive brightness temperature, deduced from observations, also shows that the transition should be inverted (for example, Berulis *et al.*, 1990).

Yet, it became a custom to consider the "broad" 4_{-1}–3_0 spectral features as "thermal" and to estimate the column density of molecules on the lower, 3_0 level, with the usual, optically thin, equation:

$$N_1 \simeq \frac{8\pi^{3/2} \cdot k \cdot v^2 \cdot (g_1/g_u)}{h \cdot c^3 \cdot A} \cdot (\Delta T_B \cdot \delta v), \tag{1}$$

where two observable quantities are: ΔT_B—the brightness temperature at line center, measured above the background, δv—the line width (FWHM), in velocity units (cm/s); and the constants are: v—the transition frequency, g_1, g_u—the statistical weights, A—the Einstein coefficient ($A = 1.5 \cdot 10^{-7}\,\text{s}^{-1}$ for 4_{-1}–$3_0\,E$ transition); other constants have their usual meanings.

Besides the assumption of the optical thickness $\tau \ll 1$, it is supposed in Eq. (1) that the absolute value of the transition excitation temperature, $|T_x|$, is $\gg hv/k$ (≈ 1.73 K for 4_{-1}–$3_0\,E$ transition), and $|T_x| \gg T_{bg}$.

From the usual solution of the radiation transfer equation,

$$\Delta T_B = (T_x - T_{bg})(1 - e^{-\tau}), \tag{2}$$

and the expression for the optical depth,

$$\tau = \frac{c^2 A (g_u/g_1)}{8\pi^{3/2} v^2 \Delta v_D} \cdot (1 - e^{-hv/kT_x}) \cdot N_1, \tag{3}$$

(where Δv_D is the Doppler width (FWHM) of the absorption coefficient) one obtains the correct expression for N_1:

$$N_1^c = \frac{8\pi^{3/2} v^2 \Delta v_D (g_1/g_u)}{c^2 A \cdot [1 - \exp(-hv/kT_x)]} \cdot \left[-\ln\left(1 - \frac{\Delta T_B}{T_x - T_{bg}}\right) \right]. \tag{4}$$

Let us introduce the reduction coefficient, C, by

$$N_1^c = N_1/C.$$

One obtains from the Eqs. (1) and (4):

$$C = \frac{k \cdot \Delta T_B}{hv} \cdot \frac{[1 - \exp(-hv/kT_x)]}{\left[-\ln\left(1 - \frac{\Delta T_B}{T_x - T_{bg}}\right) \right]}. \tag{5}$$

We see that the reduction coefficient cannot be directly obtained from the observed quantities. Besides ΔT_B, it depends on the unknown quantity T_x and on the poorly known quantity T_{bg}. The T_x can be estimated only from model calculation.

We calculated the statistical equilibrium equations for the $CH_3OH\,E$ rotational level populations in a homogeneous spherical cloud. The effects of radiation transfer in rotational lines were taken into account in a crude manner, following, in main lines, Stutzki & Winnewisser (1985), (with some modifications described by Sobolev & Kalinina ((1991), Central values method for estimation of quantum transitions excitation states with arbitrary line profile. *Astronomical and Geodesic Investigations*, Sverdlovsk, in press). Some technical details can be found in Sobolev (1990). The results—isolines of the 4_{-1}–3_0 excitation temperature, optical depth, brightness temperature at the cloud's surface, and the reduction coefficient C, are presented in Figure 10, as functions of $\lg n$ and $\lg N/\Delta v$. These are results for the model with kinetic temperature $T = 30$ K and the brightness temperature of the isotropic background $T_{bg} = 2.7$ K.
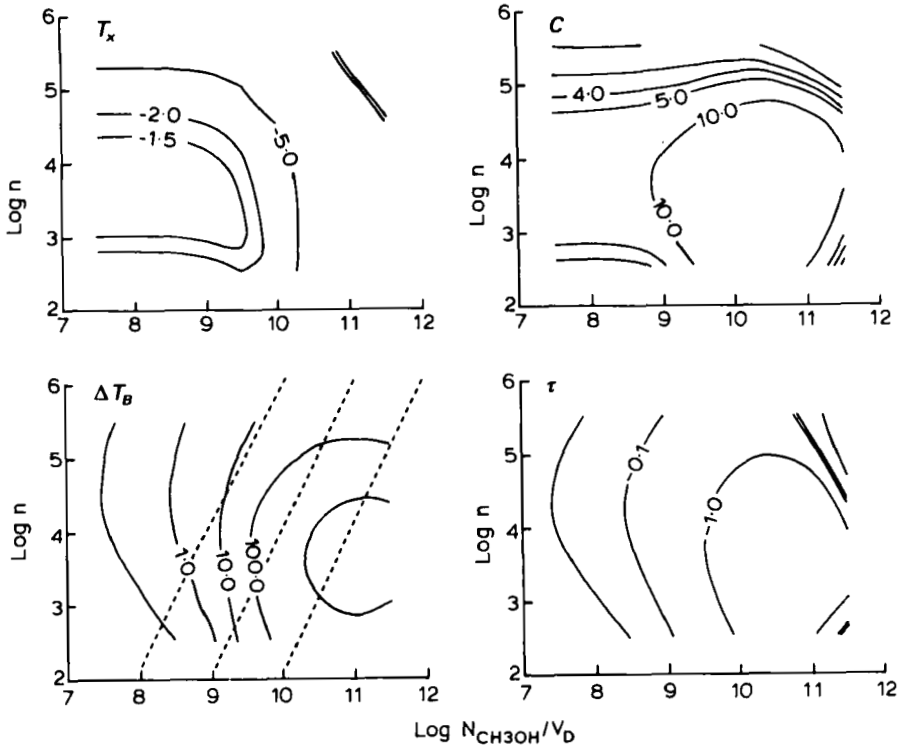
Figure 10 Isolines of the excitation temperature, T_x, optical diameter, τ, brightness temperature, ΔT_B, and reduction coefficient, C, obtained in a model simulation of the $4_{-1} - 3_0$ E line excitation in the homogeneous spherical cloud with kinetic temperature $T_k = 30$ K and isotropic background brightness temperature $T_{bg} = 2.7$ K. The isolines are presented as functions of the hydrogen number density and CH$_3$OH number density divided by velocity dispersion, both in logarithmic scale. The dashed lines on the ΔT_B graph give the field of directions according to Eq. (9). See text.

We can summarize the results as follows:

(1) In a large range of parameters, typical for the galactic molecular clouds, the 4_{-1}-3_0 transition is inverted;

(2) The assumptions underlying the Eq. (1), namely, $\tau \ll 1$, $|T_x| \gg h\nu/k$ and $|T_x| \gg T_{bg}$, could be violated in molecular clouds;

(3) Use of the Eq. (1) leads to an *overestimation* of the molecular column density—up to a factor of several tens.

The results for other models have shown a strong dependence on the assumed background continuum parameters. As a tendency, the stronger the background is, the weaker the inversion, and the smaller is the reduction coefficient C. With a sufficiently strong IR background even "anti-inversion" (overcooling) of the 4_{-1}-3_0 transition is possible.

All the column densities presented in the Table, excluding that for G1.6–0.025, were calculated using the Eq. (1) for the 3_0 level population, with subsequent transition to the total CH$_3$OH column density by applying the common partition

function. The rotational temperatures were taken: for Ori-KL from Menten *et al.* (1988), for other sources—from Menten *et al.* (1986) and Gottlieb *et al.* (1979). Thus, all the column densities in Table 1, but that for G1.6–0.025, should be regarded as upper limits and could surpass the real N values even by the order of magnitude.

The column density for the broad component of the G1.6–0.025 spectrum was estimated by a more sophisticated method of comparing the observational results for two lines, $4_{-1}-3_0$ and 2_0-3_{-1} E, with the results of a numerical modeling (Sobolev, 1990).

4.2. *The "Broad" and "Spike" Features*

One of the intriguing properties of the CH_3OH sources in $4_{-1}-3_0$ E and 7_0-6_1 A^+ lines is the coexistence of the "broad" (several km/s) and "narrow" (≤ 1 km/s) features. This was first pointed out by Morimoto *et al.* (1985), for $4_{-1}-3_0$ line in Sgr B2, and then observed by HB and HMB in this line and in 7_0-6_1 A^+ line. We also often observed this phenomenon in $4_{-1}-3_0$ E line—(see Table 1 and spectra of Sgr B2, NGC 2264, G1.6–0.025, W51, DR21 (OH)).

As we already mentioned, the high interest to the narrow-line emission in $4_{-1}-3_0$ E lines is partly due to the fact that the sources of these lines, as well as those of 7_0-6_1 A^+, $5_{-1}-4_0$ E, 8_0-7_1 A^+ and J_2-J_1 E lines ("Class A" lines), though observed in regions of active star formation, are, apparently, not connected directly with any indicators of very young stars; thus, one can suppose that they are connected with even earlier stages of star formation. It has been shown, in particular, that the J_2-J_1 E masers in Ori-KL could well be, with their observed properties, *protostars* at the stage of gravitational contraction (Strelnitskij, 1981).

Yet, before considering this intriguing interpretation for $4_{-1}-3_0$ spike features, we would like to investigate here the possibility of a more simple explanation. Namely, we will try to answer the question: may the observed superposition of the "broad" and "spike" features be due to the radiation from ordinary (not collapsing) fragments of the hierarchical structure of the interstellar medium (ISM)?

To make some quantitative estimates, we will admit that in a typical case the ratio of line widths for a "broad" and a "spike" feature is $\simeq 5$, and the ratio of their antenna temperatures is $\simeq 1$.

Let us accept the following observationally established relations between geometrical scale, L, average number density, n, and velocity dispersion, Δv, of the ISM turbulence fragments (Goldsmith & Arquilla, 1985):

$$n \propto L^{-1.2}, \tag{6}$$

$$\Delta v \propto L^{0.4}. \tag{7}$$

If we assume that the observed line width, δv, is mainly due to the turbulent velocity dispersion, that is $\delta v \simeq \Delta v$, then the adopted ratio of $\simeq 5$ for the broad and spike δv's corresponds to a dimension ratio of several tens, according to Eq. (7). Since even the broad features are not fully resolved with our antenna, the corresponding brightness temperature ratio should be $\geq 10^2-10^3$.

Taking into account that the column density, N, is equal to $n \cdot L$, we will have, from Eq. (7): $(N/\Delta v) \propto (n \cdot L \cdot L^{-0.4}) \propto (n \cdot L^{0.6})$. But, from (6) and (7):

$$n \propto \Delta v^{-3}, \tag{8}$$

and, consequently,

$$N/\Delta v \propto n^{0.5}. \tag{9}$$

The grid of dashed straight lines, superposed on the ΔT_B isolines in Figure 10, reproduces this relation. It is seen that the required transition from the observed $\Delta T_B \simeq 10^1$ K for the "broad" features to the above estimated $\Delta T_B \geq 10^3$ K for the "spikes" is possible, if the quantity $N/\Delta v$, in the clumps producing the "broad" features, is of the order 10^{10} cm^{-3} s ($\pm$ half an order), and the hydrogen number density in these clumps is of the order 10^2 cm^{-3}. Rising the density by an order, or slightly more, from this value along the dashed lines, hence, rising $N/\Delta v$ by several times only, produces the brightness temperature increase of more than two orders. This steep rise of T_B is due to a dramatic rise of the optical depth, τ, when the gas number density increases along the $N/\Delta v \propto n^{0.5}$ lines, at $N/\Delta v \simeq 10^{10}$ cm^{-3} s (see Figure 10).

Thus, the "spike" phenomenon can, in principle, be explained as a result of the transition, by decreasing the turbulence fragment dimensions, from the fragments with $|\tau| < 1$, radiating mainly spontaneous ("thermal") emission, even if the populations are inverted, to those with $|\tau| > 1$, which are subject to a real maser amplification.

This simple interpretation does not exclude, of course, that the compact fragments producing the "spike" radiation *are* collapsing protostars. More detailed investigation of the "spikes," with better resolution in space, frequency and time, is needed.

5. CONCLUSIONS

The results of the two-year regular observations of $4_{-1}-3_0$ E-methanol line in several galactic molecular clouds revealed some common properties of the sources. Superposition of the "broad" and "spike" features in the spectra and relatively stable character of radiation (including the "spike," obviously maser, emission) are to be mentioned the first.

Crude numerical calculation of the non-equilibrium level populations and the line formation in a homogeneous spherical cloud showed that the common practice of the methanol column density derivation, from the results of $4_{-1}-3_0$ E, "broad" line observations could be erroneous by the order of magnitude, due to the masing in an optically thick cloud.

Though the "spike" sources could well be compact collapsing protostars, they can also be interpreted as ordinary (gravitationally stable) fragments of interstellar turbulence, compact and dense enough ($L < 0.1$ pc, $n_H > 10^3$ cm^{-3}) to become optically thick in the inverted $4_{-1}-3_0$ line.

References

Batrla, W., Matthews, H. K., Menten, K. M. and Walmsley, C. M. (1987). Detection of strong methanol masers towards galactic HII regions. *Nature* **326,** 49–51.

Berulis, I. I. and Ponomarenko, N. I. (1988). Observations of methanol (CH_3OH) spectral line at 8-mm wavelength, In *XXI YERAC, Abstracts,* Manchester, p. 47.

Berulis, I. I., Logvinenko, S. V., Ponomarenko, N. L., Vasil'kov, V. I. and Kalenskii, S. V. (1988). Observations of 36.169 GHz ($J = 4_{-1}-3_0E$) radioline of methanol in molecular clouds. *Astron. Tsirk.* n° 1532, 19–20.

Berulis, I. I., Kalenskii, S. V. and Logvinenko, S. V. (1990). Observations of 36.169 GHz ($J = 4_{-1}-3_0 E$) radioline of methanol in molecular clouds OMC-1 and DR21 (OH). *Pis'ma v Astron. Zh.* **16,** 421–427.

Gardner, F. F. and Boes, F. (1987). *Proc. astr. Soc. Aust.* **7,** 185–188.

Gardner, F. F., Whiteoak, J. B., Forster, J. R., Peters, W. L. and Kuiper, T. B. H. (1985). Ammonia in the hot galactic center cloud G1. 6–0.025. *Proc. astr. soc. Aust.* **6,** 176–181.

Goldsmith, P. F. and Arquilla, R. (1985). Rotation in dark clouds. In *Protostars and Planets II,* D. C. Black and M. S. Matthews, eds, The University of Arizona Press, Tucson, Arizona, pp. 137–149.

Gottlieb, C. A., Ball, J. A., Gottlieb, E. W. and Dickinson, D. F. (1979). Interstellar methyl alcohol. *The Astrophys. J.* **227,** 422–432.

Haschick, A. D. and Baan, W. A. (1989). The detection of the $4_{-1}-3_0 E$ trnasition of methanol at 36.2 GHz toward hot HII regions *The Astrophys. J.* **339,** 949–955.

Haschick, A. D., Menten, K. M. and Baan, W. A. (1990). Detection of widespread strong methanol masers at 44 GHz. *The Astrophys. J.* **354,** 556–567.

Johansson, L. E. B., Andersson, C., Ellder, J., Friberg, P., Hjalmarsson, A., Höglund, B., Irvine, W. M., Olofsson, H., and Rydbeck G. (1984). Spectral scan of Orion and IRC + 10216 from 72 to 91 GHz. *Astron. Astrophys.* **130,** 227–256.

Lees, R. M. (1973). On the E_1-E_2 labelling of energy levels and the anomalous excitation of interstellar methanol. *The Astrophys. J.* **184,** 763–771.

Menten, K. M., Walmsley, C. M., Henkel, C. and Wilson, T. L. (1986). The centimeter transitions of E-type methanol. *Astron. Astrophys.* **157,** 318–328.

Menten, K. M., Walmsley, C. M., Henkel, C. and Wilson, T. L. (1988). Methanol in the Orion region. I. Millimeter-wave observations. *Astron. Astrophys.* **198,** 253–266.

Morimoto, M., Ohishi, M. and Kanzava, T. (1985). New maser lines of methanol. *The Astrophys. J. (Letters)* **288,** L11–L15.

Sobolev, A. M. (1990). Interpretation of 2_0-3_{-1} CH_3OH-E line observations in G1.6–0.025. *Astron. Tsirk.* n° 1543, 7–8.

Strel'nitskij, V. S. (1981). Interpretation of the $\lambda = 1.2$ cm methanol radio line emission in Orion. *Pis'ma v Astron. Zh.* **7,** 406–413.

Stutzki, J. and Winnewisser, G. (1985). On the interpretation of hyperfine-structure intensity anomalies in the NH_3 (J, K) = (1, 1) inversion transition. *Astron. Astrophys.* **144,** 13–26.

Whiteoak, I. B. and Peng, R.-S. (1989). Observations of 12.2 GHz methanol absorption towards the molecular cloud G1.6–0.025. *Mon. Not Roy. Astron. Soc.* **239,** 677–685.